Surfactant-assisted synthesis of Barium hexaferrite nanoparticles by hydrothermal method

Kamellia Nejati[a]*, Shabnam Alizade[b], Sara Samuey[b], Zolfaghar Rezvani*[b]

[a]Department of Chemistry, Payame Noor University, P.O. BOX 19395-3697 Tehran, Iran

[b]Department of Chemistry, Faculty of Basic Sciences, Azarbaijan Shahid Madani University, Tabriz

Abstract

In the present work, the synthesis of Barium hexaferrite ($BaFe_{12}O_{19}$) nanoparticles in the presence of a large excess amount of OH^- anions by the hydrothermal method in the presence and absence of surfactants such as sodium dodecyl benzene sulfonate and Triton X-114 was reported. The optimized temperature in the absence of surfactant was determined (200 °C) and then Barium hexaferrite nanoparticles were synthesized by assistance of surfactants at this temperature. In this way, it was confirmed that the secondary re-crystallization can be totally suppressed with the use of surfactant and addition of surfactant leads to the synthesis of uniform and ultrafine nanoparticles with excellent super paramagnetic properties. Barium hexaferite nanoparticles have a disc-like shape. The structure, morphology and magnetic properties of samples were characterized and investigated by powder X-ray diffraction (PXRD), scanning electron microscopy (SEM) and vibrating sample magnetometer (VSM) techniques.

Keywords: Barium hexaferrite; hydrothermal; surfactant; sodium dodecyl benzene sulfonate.

Introduction

In recent years, hexaferrite materials such as Barium hexaferrite with hexagonal molecular structure ($BaFe_{12}O_{19}$) were suitable candidates for industrial applications [1,2] due to

*Corresponding author: Zolfaghar Rezvani
Tel: +98 (41) 35412117, Fax: +98 (41) 35412108
E-mail: zrezvani@azaruniv.ac.ir

their high intrinsic coercivity, high curie temperature, relative large magnetization, corrosion resistivity and uniaxial magneto crystalline anisotropy and have been widely used in permanent magnets, microwave radiation adsorbents, telecommunication devices, high density magnetic recordings and magneto-optic recording media [3,4]. Recent studies have shown that physical properties of nanoparticles strongly depend on the preparation methods [5]. Various synthesis techniques such as sol–gel [6,7], auto-combustion [8], microwave-assisted sol–gel auto-combustion[9], co-precipitation [10], self-propagation high-temperature synthesis [11], carbon combustion [12], spray pyrolysis [13], aerosol pyrolysis [14] and molten salt [15] have been used or are under development for preparing ultrafine Barium hexaferrite particles. With development of nanotechnology, the hydrothermal method appeared to be quite useful for different non-materials synthesis and it was also used for preparation of small Barium hexaferrite nanoparticles without any high-temperature treatment. Since the low temperature synthesis causes poor

magnetic properties for these materials, therefore hydrothermal synthesis of uniform and ultrafine nanoparticles at higher temperatures would be of interest. Synthesis of nanoparticles at higher temperatures causes the better structural order and consequently better magnetic properties, but with increasing the temperature in the hydrothermal method, the size of nanoparticles also increases and large platelet particles appeared in the samples as a result of the secondary re-crystallization [16, 17].

For this purpose, one of the routes is using of surfactants that they can decrease the surface energy. The advantage of this method is that the solving of surfactants in the media is not necessary and also they can reduce the surface energy by placing on the surface and creating a boundary between two liquid phases and by this way it is possible to prevent the growth and aggregation of particles [18]. At the same time, the surfactant adsorbed onto the surfaces of nanoparticles provides their colloidal stability in nonpolar liquids, thus enabling the preparation of stable ferrofluids. Also the surfactant blocks the secondary re-crystallization of the nanoparticles during the

hydrothermal treatment. The secondary recrystallization or Ostwald ripening is a process in which a small number of the larger particles grow at the expense of the smaller ones. Due to very fast growth rate of these exaggerated particles, the control and decrease of particles size to the nano scale are very important and practically impossible [19,20].

In this paper, we present a method to produce Barium hexaferrite $BaFe_{12}O_{19}$ nanoparticles by assistance of sodium dodecyl benzene sulfonate and triton x-114 as surfactants and the effects of these surfactants on particle size and magnetic properties of samples have been studied.

Experimental

Materials

Analytical grade of Barium nitrate $Ba(NO_3)_2.6H_2O$ (Merck, purity 97.2%), Ferric nitrate [$Fe(NO_3)_3.9H_2O$] (Merck, purity 99.8%), sodium hydroxide NaOH (Merck, purity 99.8%), *sodium dodecyl benzene sulfonate [*$C_{12}H_{25}C_6H_4SO_3Na$], Triton X-114 [$C_{14}H_{22}O(C_2H_4O)n$] and deionized water were taken as starting materials.

Synthesis of the nanoparticles

The hydrothermal synthesis of the Barium hexaferrite was performed in a 100-mL stainless-steel autoclave cell (Parr Instruments) without any agitation. The procedure began by dissolving the appropriate amount of Barium and Iron nitrates in distilled water. The molar ratio of the precursor [Ba^{2+}]:[Fe^{3+}] was optimized at 1:5. After complete dissolution, NaOH was added to achieve the [OH^-]/[NO_3^-] ratio 16. Ultrafine hexaferrite nanoparticles can be obtained with a hydrothermal method at low temperatures by using large excess amounts of OH^- ions. Indeed, by increasing the concentration of hydroxyl (OH^-) ions relative to the metal ions (Ba^{2+} and Fe^{3+}), the formation temperature was reduced. So, the ratio of [OH^-]/[NO_3^-] was selected equal to 6 according to the literatures [19]. Then, the suspension of precipitated precursors was transferred into the autoclave and heated with a heating rate of 3 $^\circ$C min^{-1} to various temperatures ranging from 150 – 200°Cfor 5 h.The resultant precipitates were washed with distilled water and HCl (0.1 mol/L)solutionand dried in ambient air. Finally, the prepared nanoparticles at 200 °C calcined at 900 °C for 4 h.

At the second step, in order to prevent the secondary re-crystallization

of the nanoparticles during the hydrothermal treatment, Barium hexaferrite nanoparticles were synthesized in the presence of surfactants. For this purpose, 0.7 mmol(optimal value) of each surfactant (Triton x-114 or *sodium dodecyl benzene sulfonate)* was dissolved in the suspension of precipitated ferrite precursor and was heated at 200 $^\circ$C as optimal temperature resulted from XRD patterns. After hydrothermal treatment, diluted nitric acid (20%) solution was added to the suspension to decrease the pH value below 5. The decrease in pH resulted in precipitation of a hydrophobic mass composed of the synthesized surfactant-coated nanoparticles and unabsorbed surfactant. The samples were washed with acetone to remove the unabsorbed surfactant.

Characterization

To confirm the formation of a single phase, the powder X-ray diffraction patterns (XRD) of the samples were recordedwith a Bruker AXS model D8 advanced diffractometer using Cu-K radiation (= 1.542) with the Bragg angle ranging 20–70°.The average crystallite size (D) was determined using the Scherrer'sequation (1) [20],

$$D = 0.9 \ / \ \cos \theta \qquad (1)$$

Where D is the average crystalline size, the full width at half-maximum of the diffraction peak, the wave length of the X-ray (Cu-K) and θ the Bragg's angle in degrees unit. The magnetic properties were measured at room temperature, using a vibrating sample magnetometer (VSM,HH-15) in a maximum applied field of 10 kOe. A scanning electron microscope (SEM, LEO 1430VP) was employed to analyze the morphology and structure of the samples.

Results and discussion

XRD analysis

The observed changesin Purity and crystallinity of the samples with increasing temperature of the hydrothermal treatment can be detected by the XRD patterns of the samples (Figure 1a-g). All diffraction peaks are well assigned to the standard pattern of M-type $BaFe_{12}O_{19}$ crystals,reported in JCPDS card (No. 07-0267) indicating that hydrothermal route is feasible for the formation of single-phase $BaFe_{12}O_{19}$nanoparticles. The diffraction peaks at 2θ values of 30.21, 32.11, 34.11, 37.21, 40.31, 42.31, 50.31, 55.11, 56.51, and 63.11° can be assigned to the reflections of (110),

(107), (114), (203), (205), (206), (209), (217), (2011), and (220) planes of $BaFe_{12}O_{19}$, respectively. The intensity and sharpness of the mentioned peaks gradually increase by enhancing the temperature in the hydrothermal treatment from 150°C to 200 °C. This leads to an increase in the crystallite size [21,22].It should be noted that the shape of the grains and the texture of the samples can influence on the XRD patterns. Presence of large platelet crystals, which may appear in the samples treated at higher temperatures, can alter both the intensity and the shape of the peaks in XRD patterns as reported in Ref. [19].No characteristic peaks for other impurities are observed. The characteristic peaks of (hk0) plans, such as 110 and 220, are relatively sharp, while the characteristic peaks of (hkl) plans, where l 0, are broader or even missing (for lower than l). The peaks originating from the lattice planes containing l-component are broader, because of the very small dimension of the crystals along the c-direction of the hexagonal structure, which corresponds to the thickness of the nanoparticles [19]. The X-ray diffraction patterns of hydrothermally treated at 200 °C and then calcined at 900 °C sample are

shown in Figure 1g. It can be seen that with calcination of Barium hexaferrite nanoparticles, the intensity of the peaks increases and at the same time the width of the peaks decreases significantly. This confirms that the size of particles increases after the calcination.
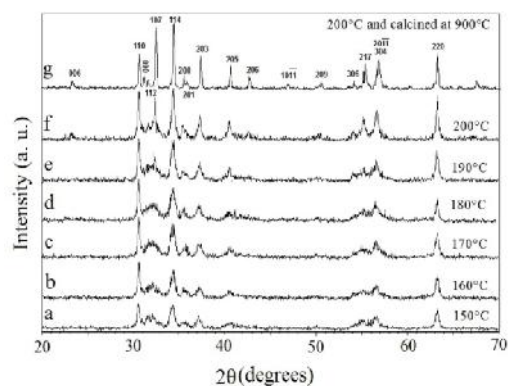

Figure1. XRD patterns of the Barium hexaferrite nanoparticles hydrothermally prepared at different temperatures (a)150 °C, (b) 160 °C, (c) 170 °C, (d) 180 °C, (e) 190 °C, (f) 200 °C, (g) 200 °C and calcined at 900 °C

Figure 2(f, h and i) shows the XRD patterns of the Barium hexaferrite nanoparticles which synthesized in the presence of sodium dodecyl benzene sulfonate and Triton x-114 as surfactant at 200 °C and also as-prepared nanoparticles synthesized without surfactant. As shown in Figure 2(h-i), the particles have a good crystallinity and also compared with Figure 2f, by adding of surfactant to suspension of

precipitated precursors of ferrite nanoparticles, the width of the peaks increases and consequently the size of particles decreases and therefore morphology of the samples improves, while the sharpness of the peaks remains relatively unchanged. Table 1 displays the average crystal sizes of all samples, calculated from the most intense peak (114) using the Scherrer's formula [23].
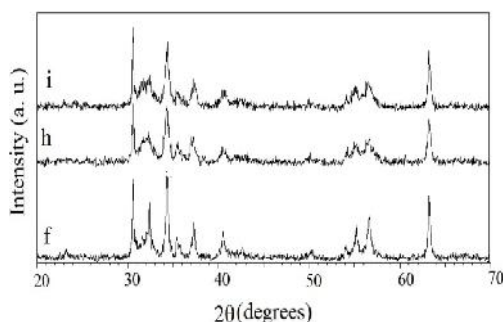

Figure 2. XRD patterns of the (f) as-prepared Barium hexaferrite nanoparticles, synthesized in the presence of (h) sodium dodecylbenzene sulfonate, (i) Triton x-114 at 200 °C

SEM analysis

In order to investigate the morphology and particle size of products, the SEM images of as-prepared Barium hexaferrite nano-particles, annealed at different temperatures, were obtained and are shown in Figure 3, a, f and g . Figure 3a shows a SEM micrograph of the nanoparticles synthesized at 150 °C.

The detailed SEM analysis revealed that the nanoparticles have a disc-like shape and uniform thickness. The disc-like nanoparticles were measured to have 25-30 nm width. Figure 3f shows a SEM image of sample prepared at 200 °C.

With increasing the temperature to 200 °C, the large platelet crystals were appeared. The comparison of Figures 3a and 3f reveals that the temperature of the hydrothermal treatment has a substantial effect on morphology and size of Barium hexaferrite nanoparticles. When the annealing temperature increases from 150 °C to 200 °C, the width and thickness of the grains increases noticeably. Figure 3g reveals that sintering of particles leading to massive, agglomeration and sintered particles has no clear boundary. Figure 4, h and i, shows the SEM micrographs of Barium hexaferrite nanoparticles, which synthesized at the presence of sodium dodecyl benzene sulfonate and Triton x-114 at 200 °C. In both Figures 4h and 4i, Barium hexaferrite nanoparticles have disc-like shape, but in the presence of Triton x-114, the smaller and uniform crystals have been formed.

Table 1. Average crystallite size of Barium hexaferrite nanoparticles, prepared with and without surfactants at different temperatures

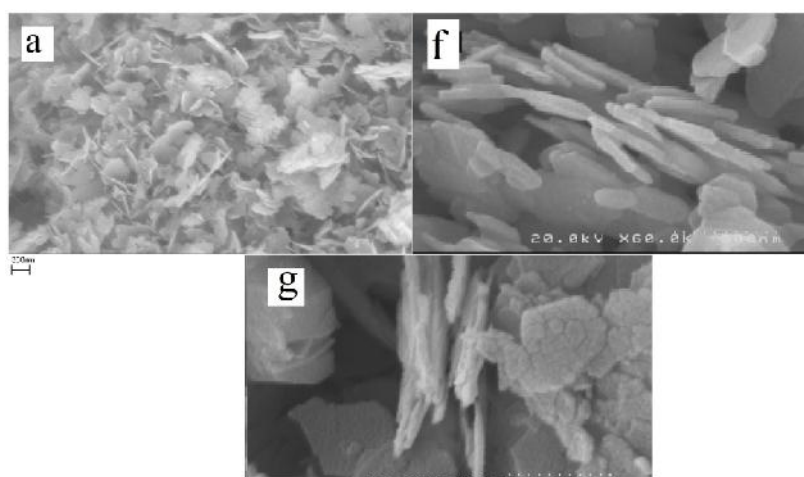| Sample	Tempreture (^oC)	surfactant	D (nm)
a	150	-	21
f	200	-	38
g	900	-	90
h	200	sodium dodecyl benzene sulfonate	24
i	200	Triton X-114	17

Figure 3. The SEM images of Barium hexaferrite nanoparticles hydrothermally synthesized at (a) 150 °C (f) 200 °C and (g) 200 °C followed by calcination at 900 °C

By comparing Figures 3 and 4 of the synthesized Barium hexaferrite nanoparticles, without and with the surfactant, it can be deduced that in the absence of surfactant, increasing the temperature to 200 ^oC, leads to the appearance of the product in the form of the large platelet grains. The mentioned large platelet crystals are the result of secondary re-crystallization (Ostwald ripening). While by using surfactants in the synthesis process, particles size decreases very slowly. The surfactant causes the consuming of all the precursors for formation of hexaferrite and there by the growth of the hexaferrite nanoparticles islimited after nucleation [19]. Thus, we can successfully suppress the secondary re-crystallization during the hydrothermal

synthesis of Barium hexaferrite nanoparticles by using surfactants. It can be seen from the Figure 4 that Triton x-114 decreases particles size more than sodium dodecyl benzene sulfonate. All of these results confirm the previous results of the XRD patterns.

VSM analysis

Figure 5, a-b, shows the hysteresis loops obtained from VSM measurements for Barium hexaferrite samples at room temperature under an applied field of 10 kOe. The coercivity(Hc), squareness ratio (Mr/Ms), saturation magnetization (Ms) and remanent magnetization (Mr) of nanoparticles are given in Table 2. According to the Figure 5a and Table 2, it can be seen that the saturation magnetization and the coercivity of synthesized sample at 150 °C (sample

a) are 13.39 emu/g and 307.45Oe respectively, while for sample f, prepared at 200 °C, the saturation magnetization and the coercivity are 23.89 emu/g and 916.92Oe respectively. This suggests that the magnetization and coercivity of the samples strongly increase by increasing the temperature. Since by increasing the temperature of the treatment, the particle size and the number of large platelet crystals increase; therefore the increasing in magnetization and coercivity can be mainly related to the number of large platelet crystals [18]. The results show that the saturation magnetization is still much lower than the theoretical value of BaM single crystal, but a little higher than or similar to the reported results in literatures [24].
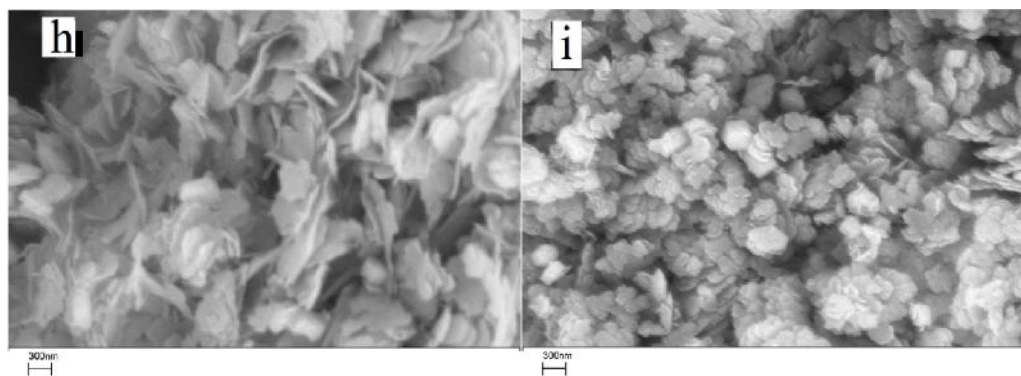

Figure 4. The SEM micrographs of the Barium hexaferrite nanoparticles synthesized in the presence of, (h) Sodium dodecyl benzene sulfonate, (i) Triton x-114 at 200 °C
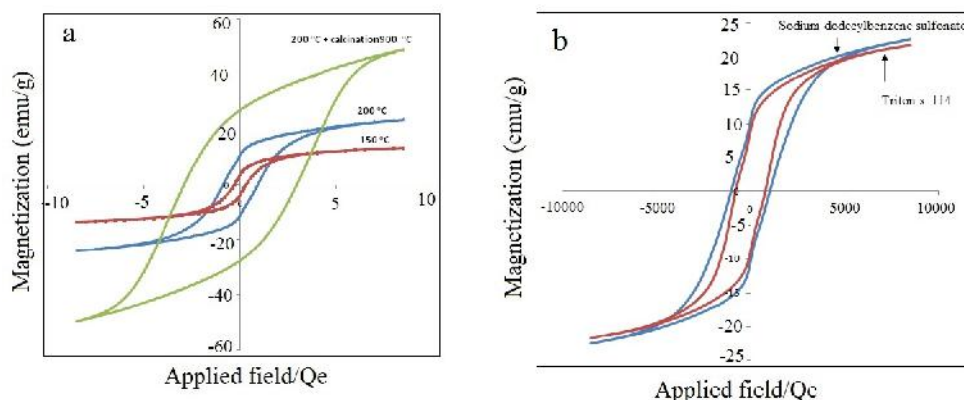
Figure 5. a) Magnetic hysteresis loops of the Barium hexaferrite nanoparticles hydrothermally synthesized at 150 °C, 200 °C and 200°C followed by calcination at 900 °C, b) Magnetic hysteresis loops of the Barium hexaferrite nanoparticles synthesized in the presence of, sodium dodecyl benzene sulfonate and Triton x-114

Table 2. The observed values of coercivity Hc, squareness ratio (Mr/Ms), saturation magnetization (Ms) and remanent magnetization (Mr) of Barium hexaferrite nanoparticles

Smple	Tempretu re (^{o}C)	Surfactant	D (nm)	Ms (emu/g)	Mr (emu/g)	Mr/Ms	Hc (Oe)
a	150	–	21	13.39	3.609	0.2695	307.45
f	200	–	38	23.89	10.90	0.4577	916.92
g	900	–	90	50.10	27.21	1.95	2970.7
h	200	SDBS[a]	24	22.57	10.48	0.4645	1036
i	200	Triton X-114	17	21.75	8.92	0.41	758

[a]Sodium dodecyl benzene sulfonate

The incomplete coordination of atoms on the particle surface can cause the reduction of the magnetization of the magnetic particles, leading to a no collinear spin configuration, which reduces the magnetization of the particles by formation of a surface spin coating [25, 26]. Moreover, the thermal fluctuation of the magnetic moments can significantly diminish the total magnetic moment at a given magnetic field [27]. Typically, the single-domain

$BaFe_{12}O_{19}$ nanoparticles, that prepared by other soft chemical methods, reveal coercivities of 4000 Oe and more [28-31].

The size of prepared samples was generally smaller than the critical diameter for domain formation in $BaFe_{12}O_{19}$, which was expected to be around 1 μm [32, 33]. Therefore, the low coercivity values are related not only to the domain formation, but also to the high shape anisotropy of the samples resulting from their high width-to-thickness ratio. For example, the coercivity linearly depends on the magnetocrystalline anisotropy and the shape anisotropy, and in the $BaFe_{12}O_{19}$ platelets, two anisotropy fields oppose each other [34]. Moreover, the crystalline order in the *c*-direction in thin platelet crystals may be very lowand can also have an opposite effect on the coercivity. The hysteresis loop of the sintered Barium hexaferrite at 900 °C shows that by sintering of the sample, the values of saturation magnetization (Ms), remanent magnetization (Mr) and coercivity (Hc) increase, due to increasing in crystal sizes.

Figure 5b shows the magnetic properties of the Barium hexaferrite samples, synthesized in the presence of sodium dodecyl benzene sulfonate and Triton X-114. It can be seen from the Figure that the magnetic properties of synthesized nanoparticles at the presence of surfactants are not much different from the samples prepared at the absence of surfactants. Although, the size of the nanoparticles slowly decreases in the presence of surfactants, but the improvement in the magnetic properties can mainly be related to the increase in their crystalline order [17]. The comparison of the effects of two surfactants on the magnetic properties of samples shows that the magnetic properties of synthesized nanoparticels at the presence of Triton X-114 are lower than that of Sodium dodecyl benzene sulfonate. The squareness ratio (Mr/Ms) of these samples is found to be lower or around 0.5, which is equal to the value expected for randomly packed single-domain particles [16].

However, this squareness ratio for sintered sample at 900 °C is more than 0.5 which can be due to single domain formation.

Conclusion

In the present work, the single phase $BaFe_{12}O_{19}$ nanoparticles have been successfully synthesized by a

hydrothermal method at different temperatures and also the effect of various temperatures on the particle size and magnetic properties were investigated. According to the results, the enhancement of temperature of the hydrothermal treatment leads to the increasing of magnetic properties and the size of particles. In this study, the effects of surfactants have been studied and were observed that surfactants enable the synthesis of uniform and ultrafine nanoparticles and also undesired process of secondary re-crystallization can be totally suppressed by this method.

Acknowledgements

References

[1] R. Sharma, R.C. Agarwala, V.A. Garwala, *Materials Letters*, **2008**, *62*, 2233–2236.

[2] F.Z. Song, X.Q. Shen, J. Xiang, Y.W. Zhu, *J Alloys Compd*., **2010**, *507*, 297–301.

[3] D. Bahadur, S. Rajakumar, A. Kumar, *J. Chem. Sci*., **2006**, *118*, 15–21.

[4] Q. Mohsen, *Am. J Appl. Sci*., **2010**, *7*, 914-921.

[5] C.R. Gong, G.L. Fan, C.L. Song, *Trans Tianjin Univ*., **2007**, *13*, 117–120.

[6] T.S. Candac, E.E. Carpenter, C.J. O'Connor, V.T. John, S. Li, *IEEE Trans Magn*., **1998**, *34*, 1111–1113.

[7] V. Pillai, P. Kumar, M.J. Hou, P. Ayyub, D.O. Shah, *Adv Coll Int Sci*., **1995**, *55*, 241–269.

[8] Y. Li, Q. Wang, H. Yang, *Curr. Appl. Phys*., **2009**, *9*, 1375–1380.

[9] M.J. Iqbal, A. Barkat-ul, *Mater. Sci. Eng. B, Solid-State Mater. Adv. Technol*., **2009**, *164*, 6–11.

[10] N.J. Shirtcliffe, S. Thompson, E.S. O'Keefe, S. Appleton, C.C. Perry, *Mater. Res. Bull*., **2007**, *42*, 281–287.

[11] Y. Liu, M.G.B. Drew, J. Wang, M. Zhang, *J. Magn. Magn. Mater*., **2010**, *322*, 366–374.

[12] M.M. Rashad, M. Radwan, M.M. Hessien, *J. Alloys Compd*., **2008**, *453*, 304–308.

[13] L. You, L. Qiao, J. Zheng, M. Jiang, L. Jiang, J. Sheng, *J. Rare Earths*., **2008**, *26*, 81–84.

[14] K.S. Martirosyan, E. Galstyan, S.M. Hossain, Y.J. Wang, D. Litvinov, *Mater. Sci. Eng. B*., **2011**, *176*, 8–13.

[15] M.H. Kim, D.S. Jung, Y.C. Kang, J.H. Choi, *Ceram. Int*., **2009**, *35*, 1933–1937.

[16] S. Singhal, A.N. Garg, K. Chandra, *J. Magn. Magn. Mater*., **2005**, *285*, 193–198.

[17] J. Yu, S. Tang, L. Zhai, Y. Shi, Y. Du, *Physica B*., **2009**, *404*, 4253–4256.

[18] L. Du, Y.C. Du, Y. Li, J.Y. Wang, C. Wang, X.H. Wang, P. Xu, X.J. Han, *J. Phys. Chem C*., **2010**, *114*,19600–19606.

[19] D. Primc1, D. Makovec1, D. Lisjak, M. Drofenik, *Nanotechnology*, **2009**, *20*, 315605-315613.

[20] K. Sadhana, K. Praveena, S. Matteppanavar, B. Angadi, *Appl. Nanosci*., **2012**, *2*, 247–252.

[21] T. Wejrzanowski, R. Pielaszek, A. Opalin´ ska, H. Matysiak, W. Lojkowski, K.J. Kurzydlowski, *Appl. Surf. Sci*., **2006**, *253*, 204-208.

[22] R. Pielaszek, Analytical expression for diffraction line profile for polydispersive powders Applied Crystallography Proceedings of the XIX Conference., **2006**, 43-50.

[23] B. Shirk, W. Buessem, IEEE Trans Magn.**1971**, *7*,659–663.

[24] M. Pal, S. Bid, S.K. Pradhan, B.K. Nath, D. Das, D. Chakravorty, J. *Magn Magn Mater*., **2004**, *269*,42–47.

[25] J. Coey, *Phys. Rev. Lett*., **1971**, *27*, 1140-1142.

[26] R. Kadama, A. Berkowitz, E. McNiff, S. Foner, *Phys. Rev. Lett*., **1996**,*77*, 394-397.

[27] A. Mali, A. Ataie, *J Alloys Compd*., **2005**, *399*, 245–50.

[28] J. Huang, H. Zhang, W. Li, *Mater Res Bull*., **2003**, *38*, 149–59.

[29] A. Mali, A. Ataie, *Ceram Int*., **2004**, *30*, 1979–83.

[30] A. Mali, A. Ataie, *Scripta Mater*., **2005**, *53*, 1065–1070.

[31] S. Li, IEEE Trans Magn., **1986**, *22*,14–18.

[32] E. Stoner, E. Wohlfarth, *J. Math. Phys. Sci*., **1948**, *240*, 74-78.

[33] J. Went, G. Rathenau, E. Gorter, G. Van Oosterhout, *Philips Tech. Rev*., **1952**,

13, 194–208.

[34] O. Kubo, T. Ido, H. Yokoyama, IEEE Trans. Magn., **1982**, *18*, 1122–1124.